Magnetostatic Calculations for 1986-7 Tohoku Bubble Chamber Magnet

Robert C. Sanders

November 19, 1986

1 Calculations Procedure—Using TRIM

Computer calculations of the magnetostatic field of the 1986 Tohoku Bubble Chamber magnet were made using TRIM. Since TRIM is a two-dimensional program, the magnet was modeled as having cylindrical symmetry about the Bubble Chamber axis. Figure 1 illustrates the orientation of the magnet coil and yoke with respect to the Bubble Chamber axis and beam centerline. The coils have cylindrical symmetry, but the iron yoke does not, and its shape was distorted for the computer model.

Figures 2-5 show the actual vertical cross section of the iron yoke at different distances from the beam centerline. The magnet has two identical halves, and it does not matter in what direction along the beam axis this distance is measured. In these figures small chamfers, bevels, boltholes and the like are ignored. On each figure is listed the cross sectional area of the iron for that region. The computer model was derived by "smearing" each iron cross section into an annular shape symmetric about the Bubble Chamber axis, keeping the cross sectional area the same. For example, Fig. 6 shows how the cross section in Fig. 2 was modeled. Figure 7 shows one-quarter of the horizontal cross section of the assumed magnet geometry. One-half of the magnet can be imagined by rotating all points in the graph on Fig. 7 completely about the Z, or Bubble Chamber, axis. The other half

of the magnet is identical. In Fig. 8 is the model for the 1985 magnet derived by Wes Craddock, using the same procedure. Table 1 has the B-H data used for the iron in both Craddock's calculations and mine.

Because of high axial forces predicted for the 1986 geometry, calculations were made for possible modifications of the magnet geometry. The modifications were made by increasing the air gap between the coil and region 7 of Fig. 7 by 2″, 3″, 4″, and 6″. This was achieved by increasing the length of region 10 in Fig. 7 by the necessary amount.

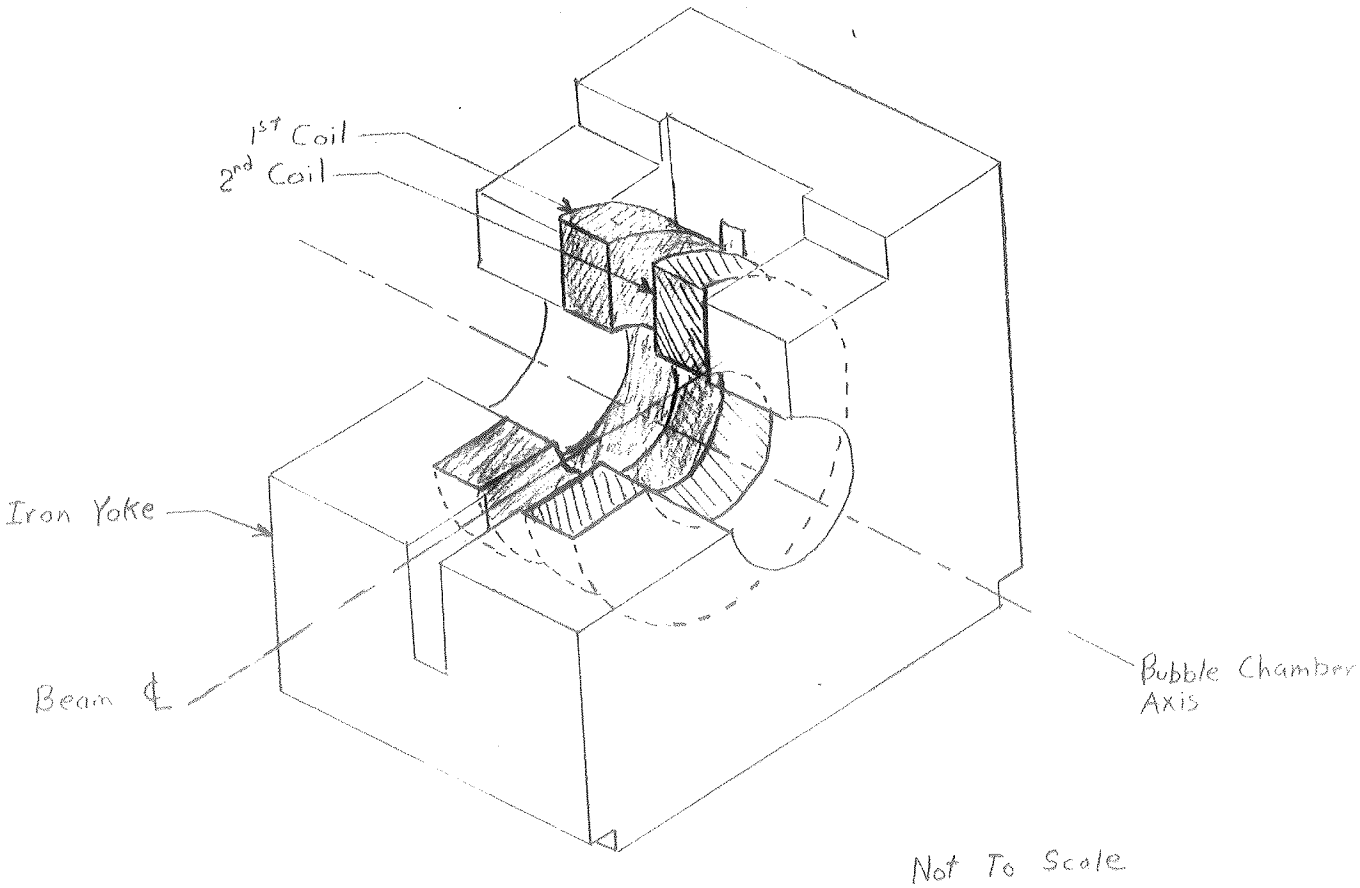

Figure 1: This sketch shows the Tohoku Bubble Chamber magnet with part of the iron cut away to expose the coils. One coil, in its cryostat, has its exposed portions shaded,and the other is crosshatched. This sketch is to show the position of the iron yoke and the coils with respect to the Bubble Chamber axis and beam centerline; the dimensions are distorted and detail is glossed over.

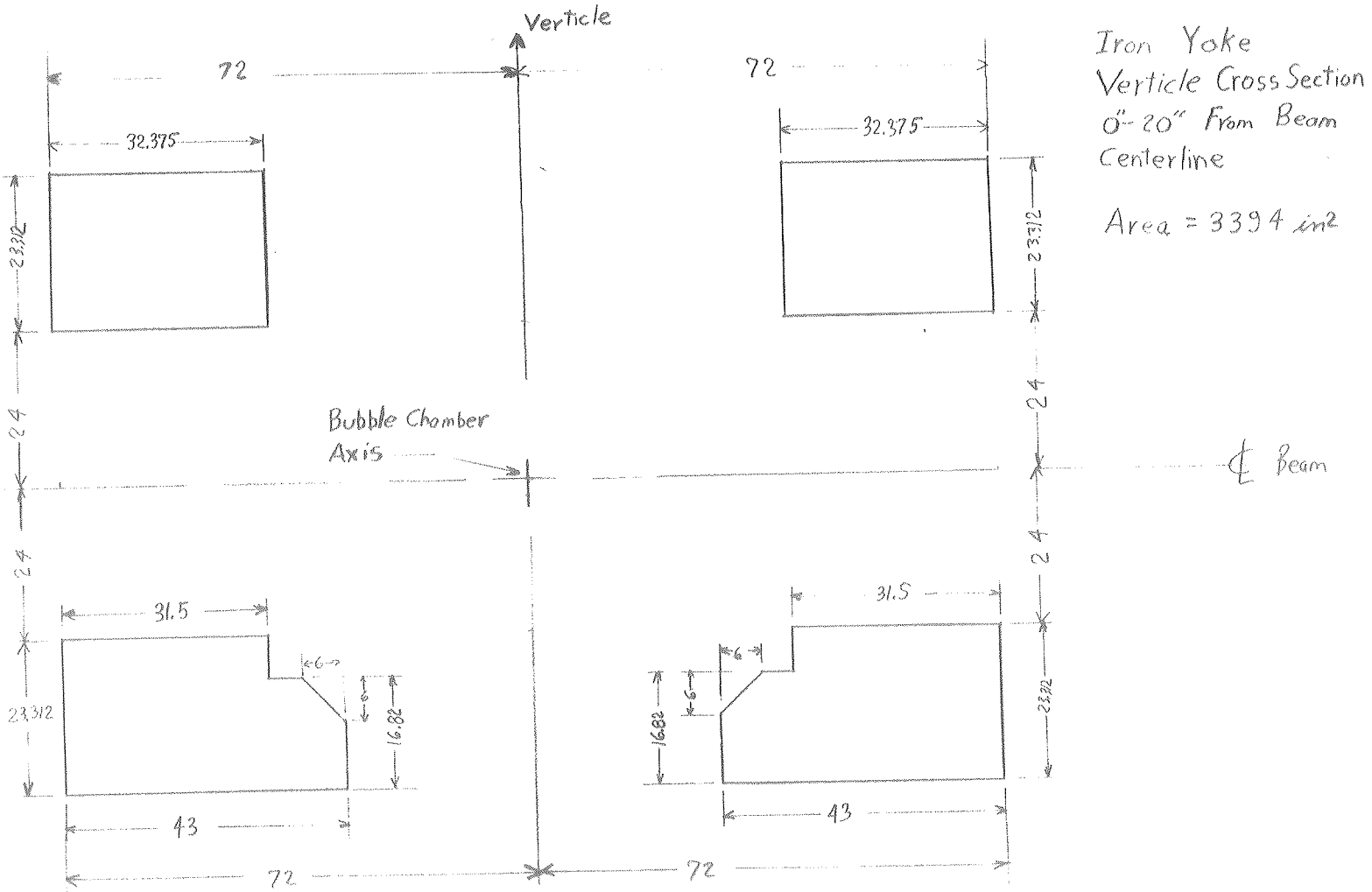

Figure 2: Tohoku Bubble Chamber Iron Yoke

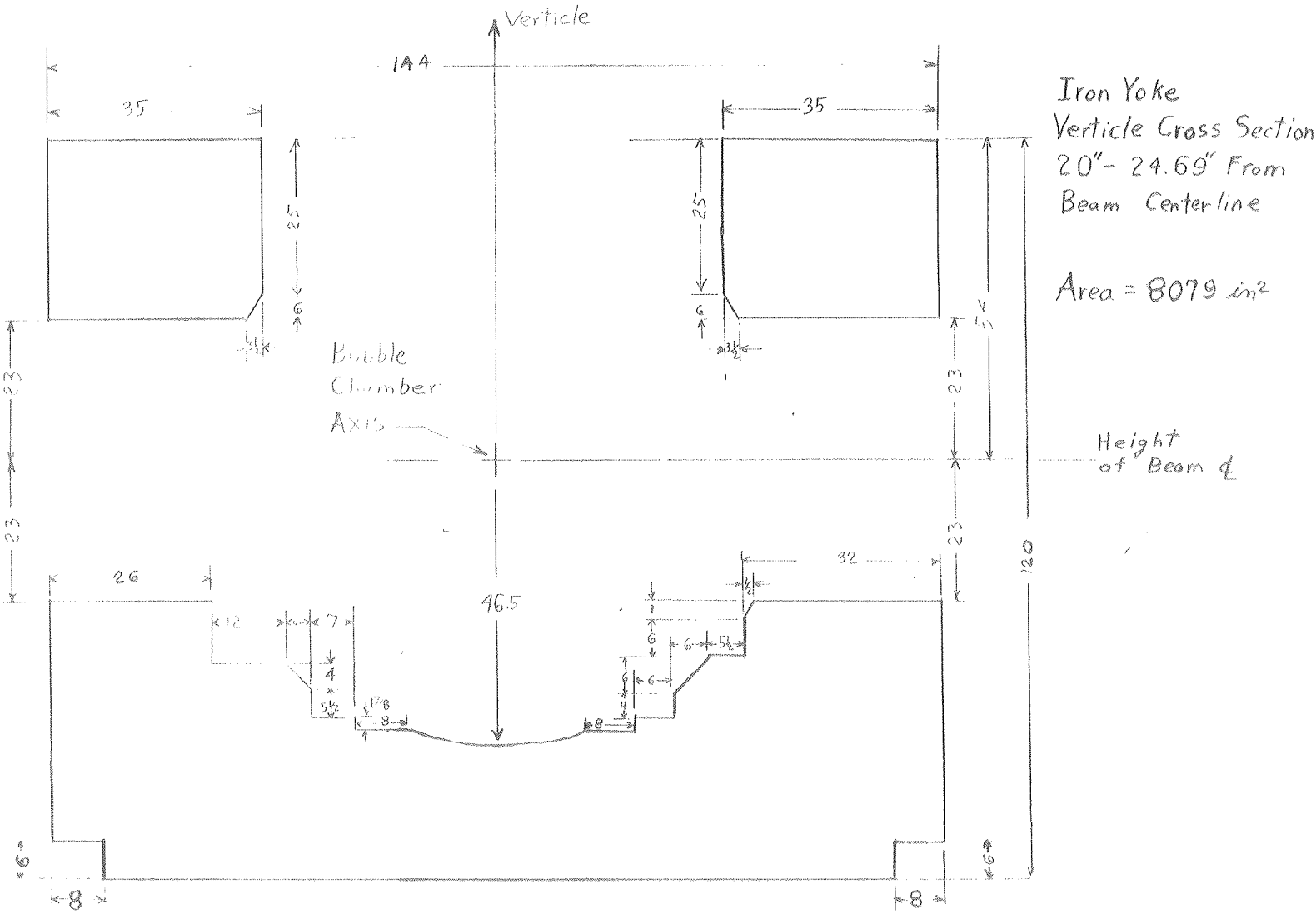

Figure 3: Tohoku Bubble Chamber Iron Yoke

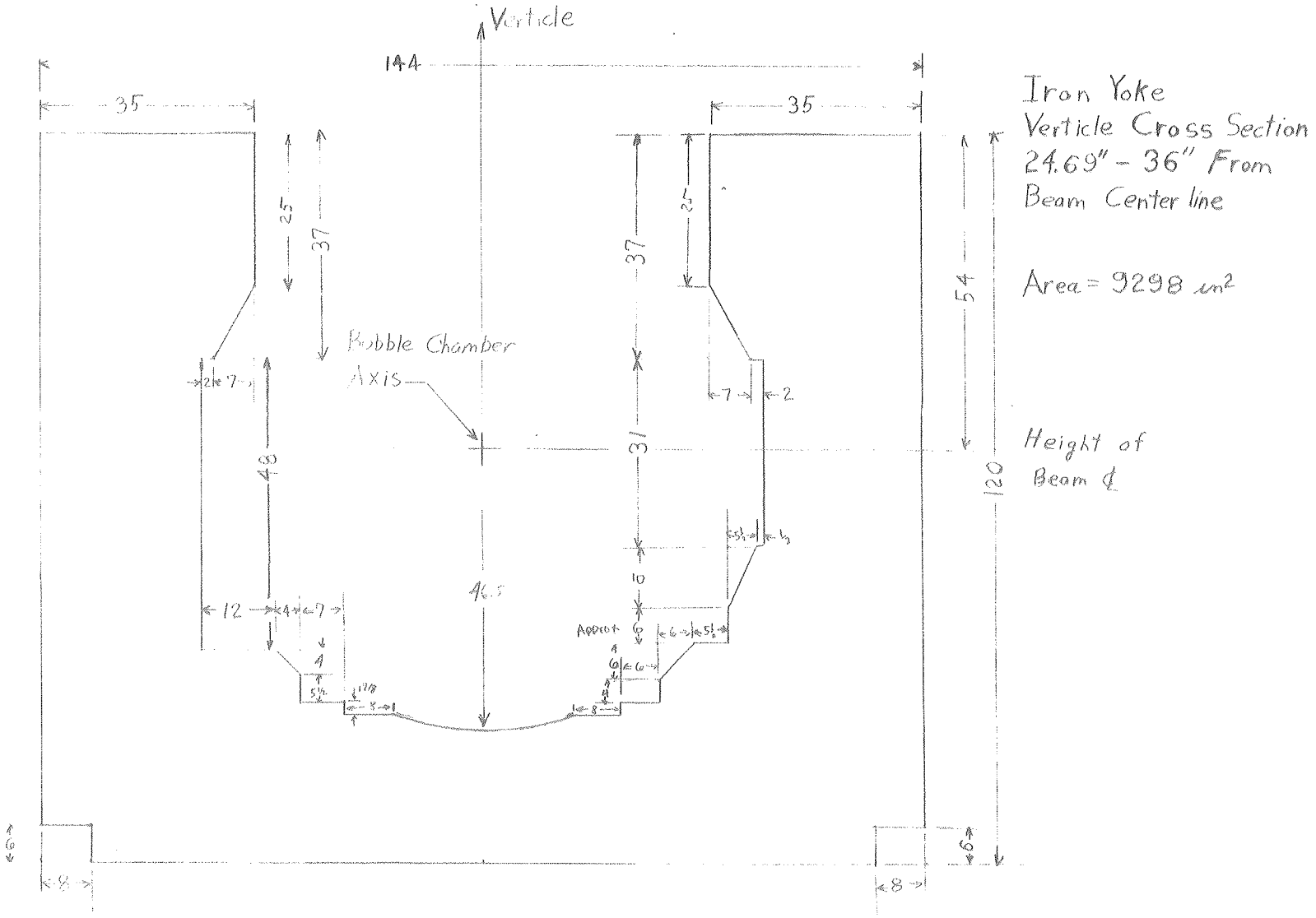

Figure 4: Tohoku Bubble Chamber Iron Yoke

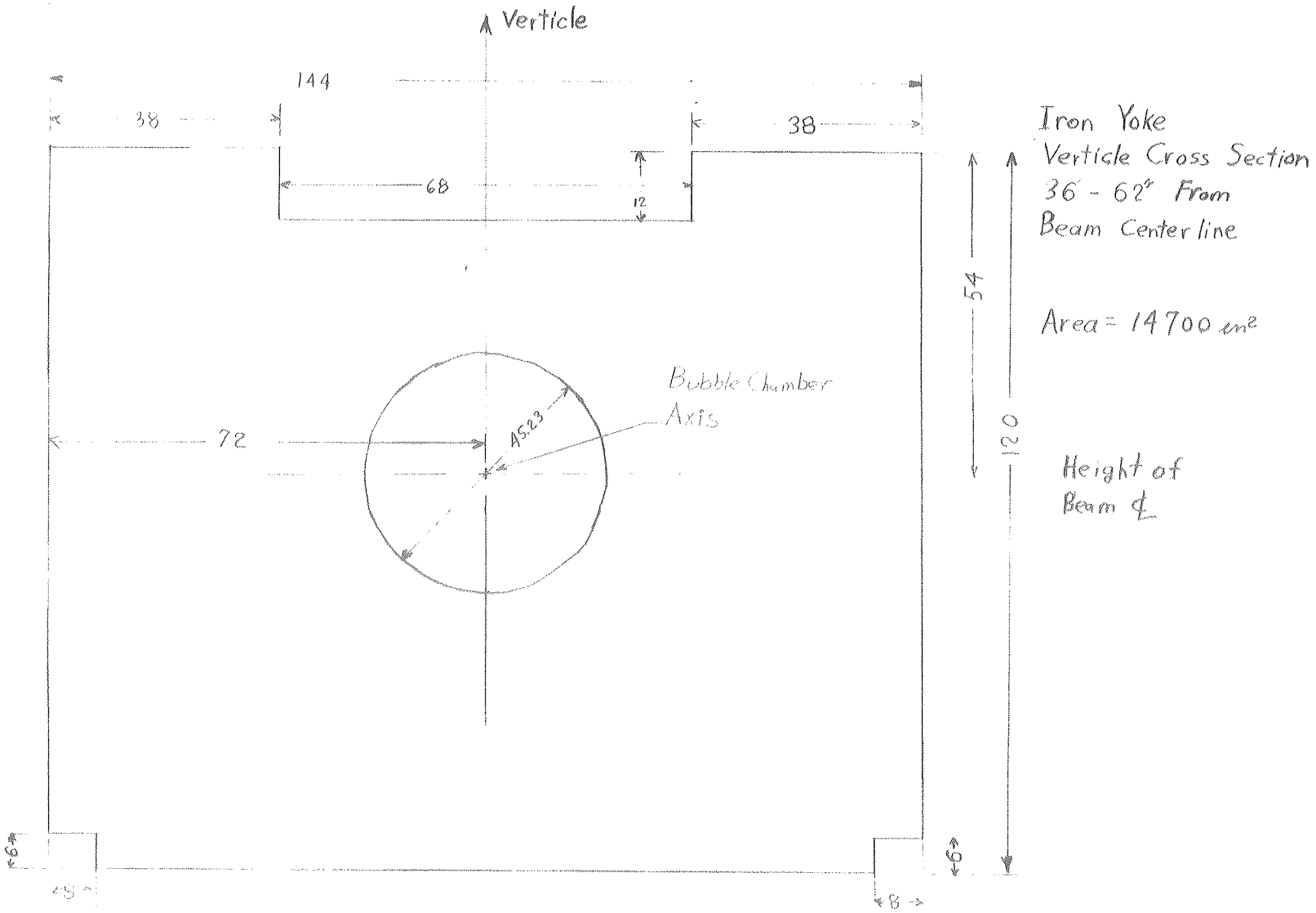

Figure 5: Tohoku Bubble Chamber Iron Yoke

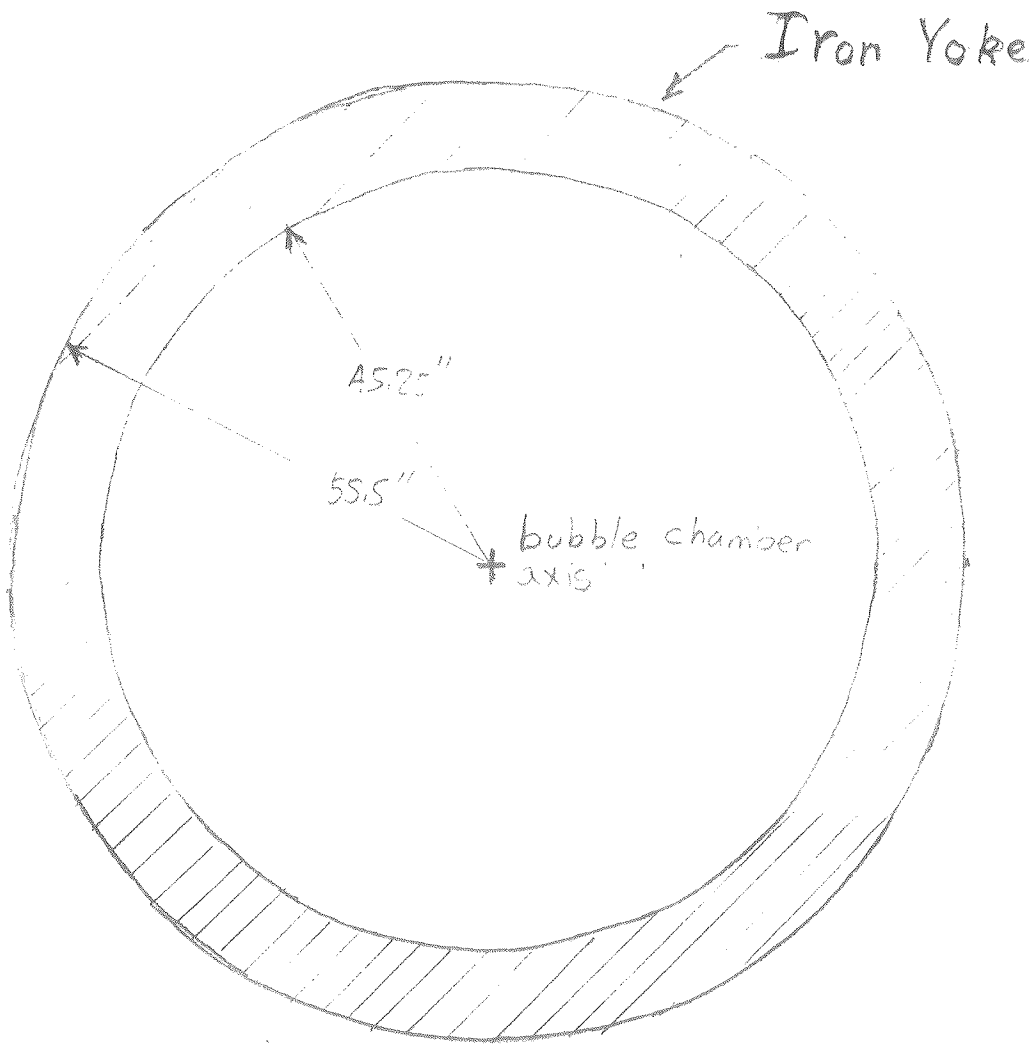

Figure 6: Assumed geometry of vertical cross section of iron yoke in the region 0-20″ from the beam centerline. This corresponds to the actual geometry in Fig. 2.

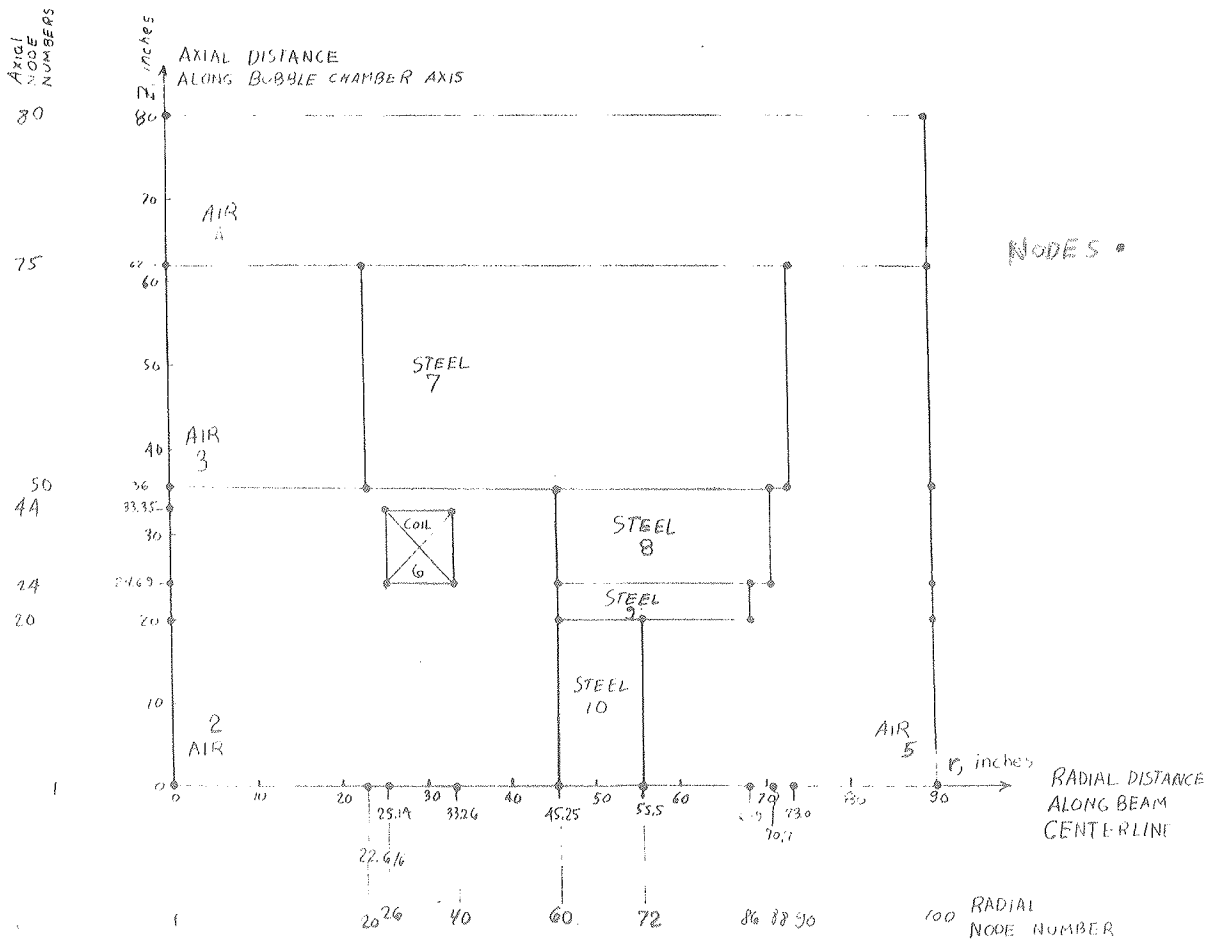

Figure 7: One quadrant of the horizontal cross section of the assumed geometry for the 1986 magnet. Also, for reference only, is shown the region numbers, specified node locations and nodal coordinates used in the input file for TRIM. This was used in RNTRIM61.

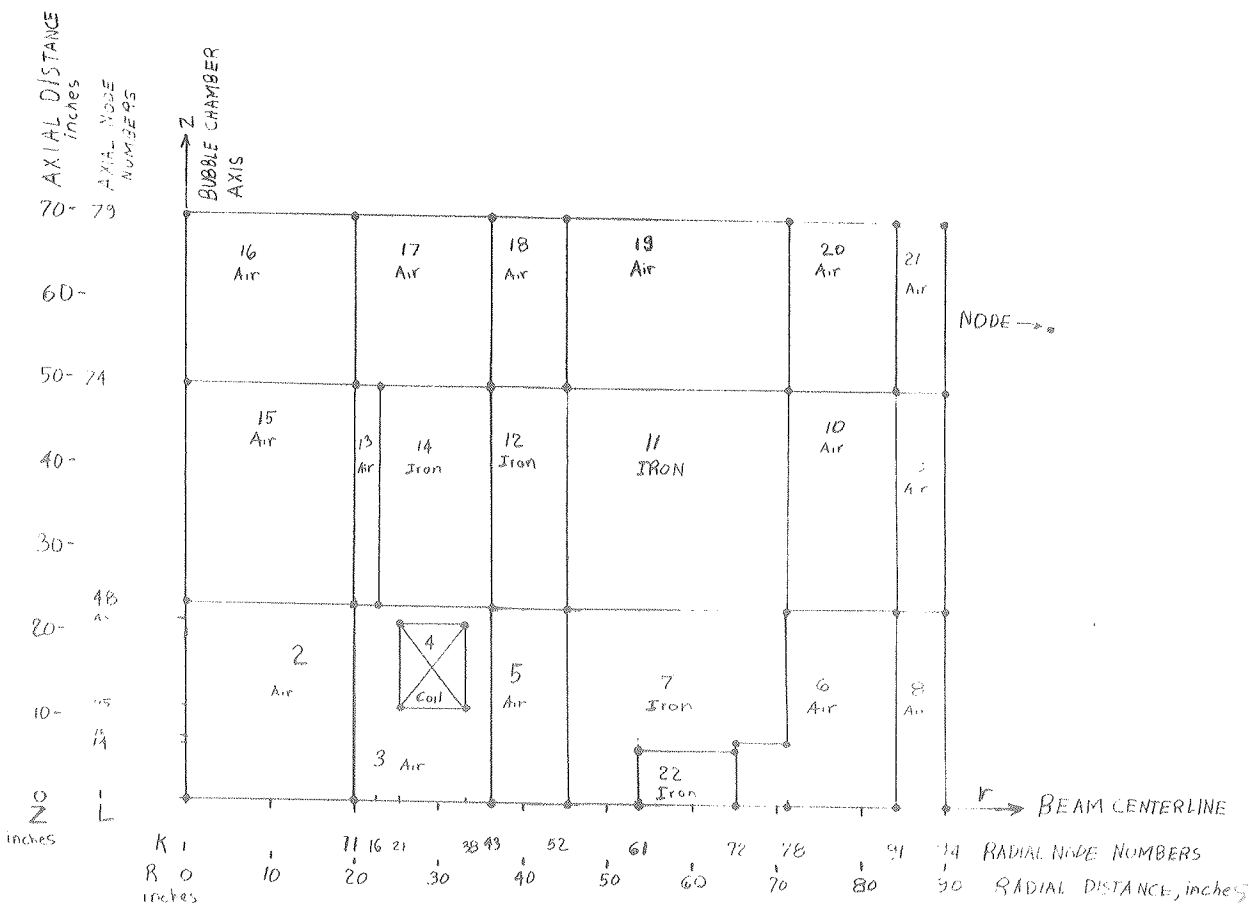

Figure 8: One quadrant of the horizontal cross section of the assumed geometry for the 1985 magnet, derived by Wes Craddock. Also, shown for reference only, is the region numbers, specified node locations, and nodel coordinates used in the input file for TRIM. This was used in RNTRIM47.

Table 1: B-H Data Used in TRIM Calculations

B(Kilogauss)	H(Oersteds)
0.000	0.000
12.000	3.696
14.000	6.300
15.000	10.000
15.492	14.485
16.000	22.560
16.500	35.070
17.000	55.080
17.499	75.944
18.000	102.060
18.493	132.966
19.000	171.000
19.500	216.450
20.000	266.000
20.500	336.200
21.000	424.200
21.250	480.249
21.500	550.400
21.750	659.023
22.000	829.400
22.500	1249.987
22.797	1519.780
23.069	1774.505
23.443	2131.179
23.996	2666.178
24.905	3557.853
25.627	4271.203
26.706	5341.188
28.498	7124.527
32.074	10691.188
42.782	21391.199
121.400	100000.000

2 Magnetic Field

Figure 9 is a plot of the central field $B_Z(0,0)$ as a function of current for the different magnets. There is a substantial difference in the central field between the 1985 and 1986 magnets. This is to be expected since the air gap offers far more resistance to the magnetic flux than the iron, and the 1986 magnet has a much larger air gap than the 1985 magnet. This results in the 1986 magnet having a much lower central field than the 1985 magnet for the same current. Also the various possible modifications of the 1986 magnet show only a modest 15% or less change in the central field, which again is comparable to the changes in the size of the air gap. Figure 10 shows a graph of stored magnetic energy versus current for the 1985 magnet and the 1986 magnet with the 6″ additional gap. The changed geometry has little effect on the stored energy.

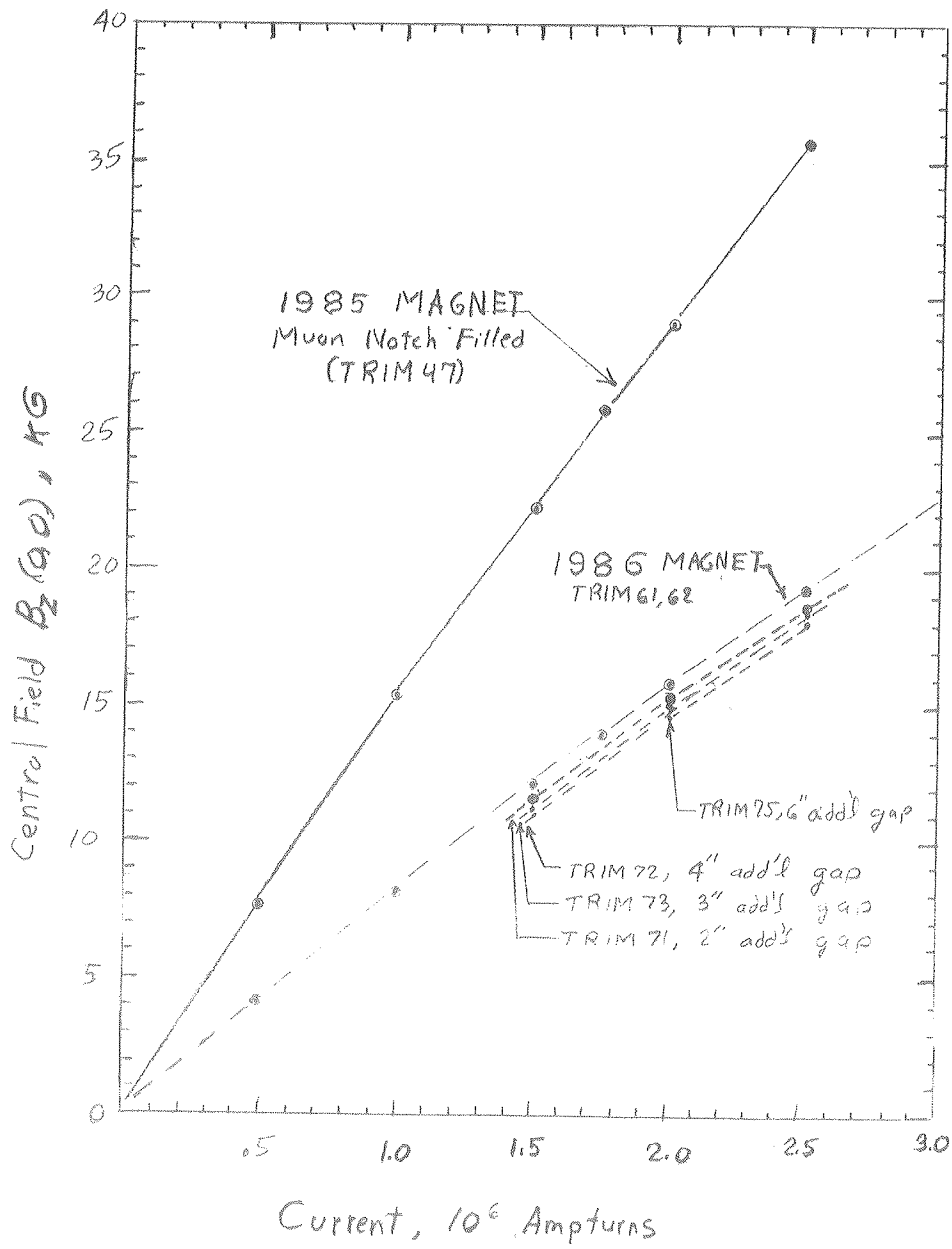

Figure 9: Central field versus current for the different magnet geometries.

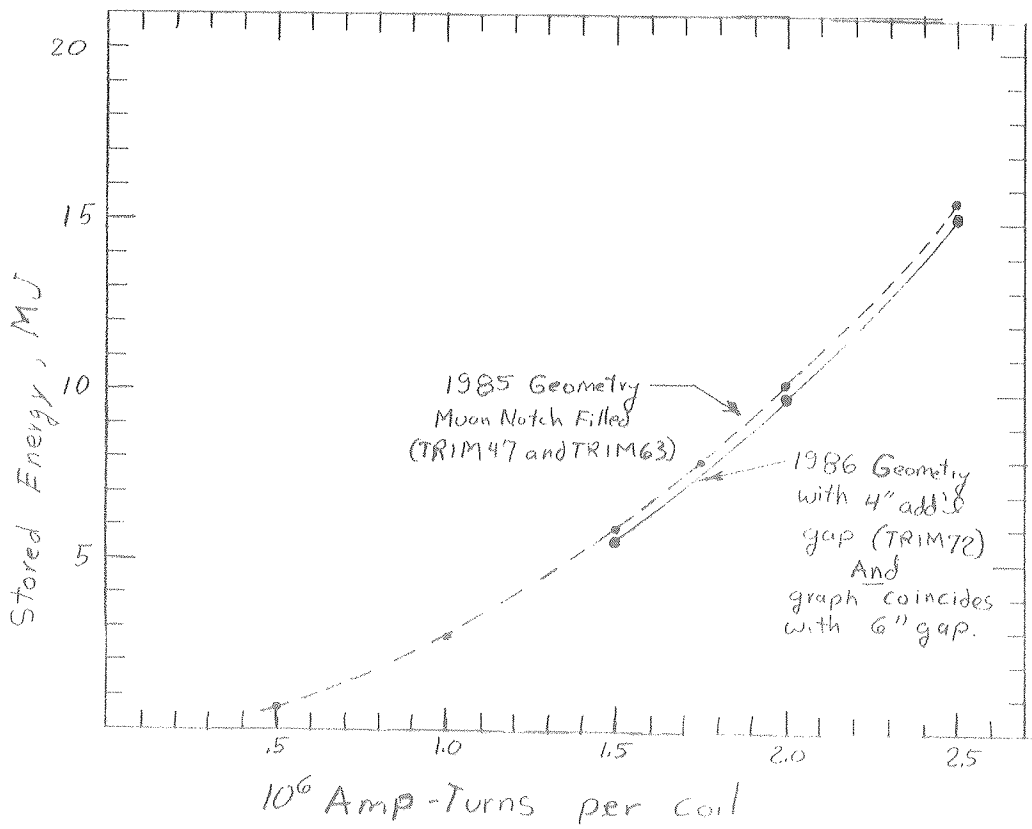

Figure 10: Stored energy for the 1985 magnet and the different variations of the 1986 magnet.

3 Axial Forces

Axial forces on the coil were calculated using FORGY, a companion program to TRIM. Figure 11 shows a graph of axial force, F_Z, versus current for the different iron configurations. The force F_Z is acting away from the center of the magnet. One component of this axial force is an attraction between the coils, which pushes each coil towards the center of the magnet. This attraction can be analytically calculated, since the coils are solenoids. The details of the calculations are in Appendix A, and results for the 1985 and 1986 magnets are in Fig. 12. The various modifications of the 1986 magnet have the same curve as the 1986 magnet. Obviously one of the reasons for lower axial forces in the 1985 magnet is the larger attraction between the coils.

The other principle component to the axial force is the attraction of the coil to the iron in region 7 of Fig. 7, which is the cross section shown in Fig. 5. The attraction of the coil to the other iron in the return legs of the iron yoke has a much smaller axial component. For convenience I will call this attractive force to the iron F_I, which is obtained by adding the attractive force between the coils to the total force F_Z on the coil. Fig. 13 is a graph of F_I for the 1985 and 1986 magnets versus current. Due to the higher fields, the iron in the 1985 magnet is more saturated than that in the 1986 magnet, thus helping to explain the lower values of F_I for the 1985 magnet.

Figure 14 has F_I plotted versus $1/y$, where y is the distance between the iron and midpoint of the coil for the different variations of the 1986 magnet. This shows that F_I is proportional to $1/y$ for a given current. Also by extrapolating the data with a straight line, it is seen that F_I approaches 0 as y gets larger. This supports the contention that F_I is primarily due to the attraction between the coil and the

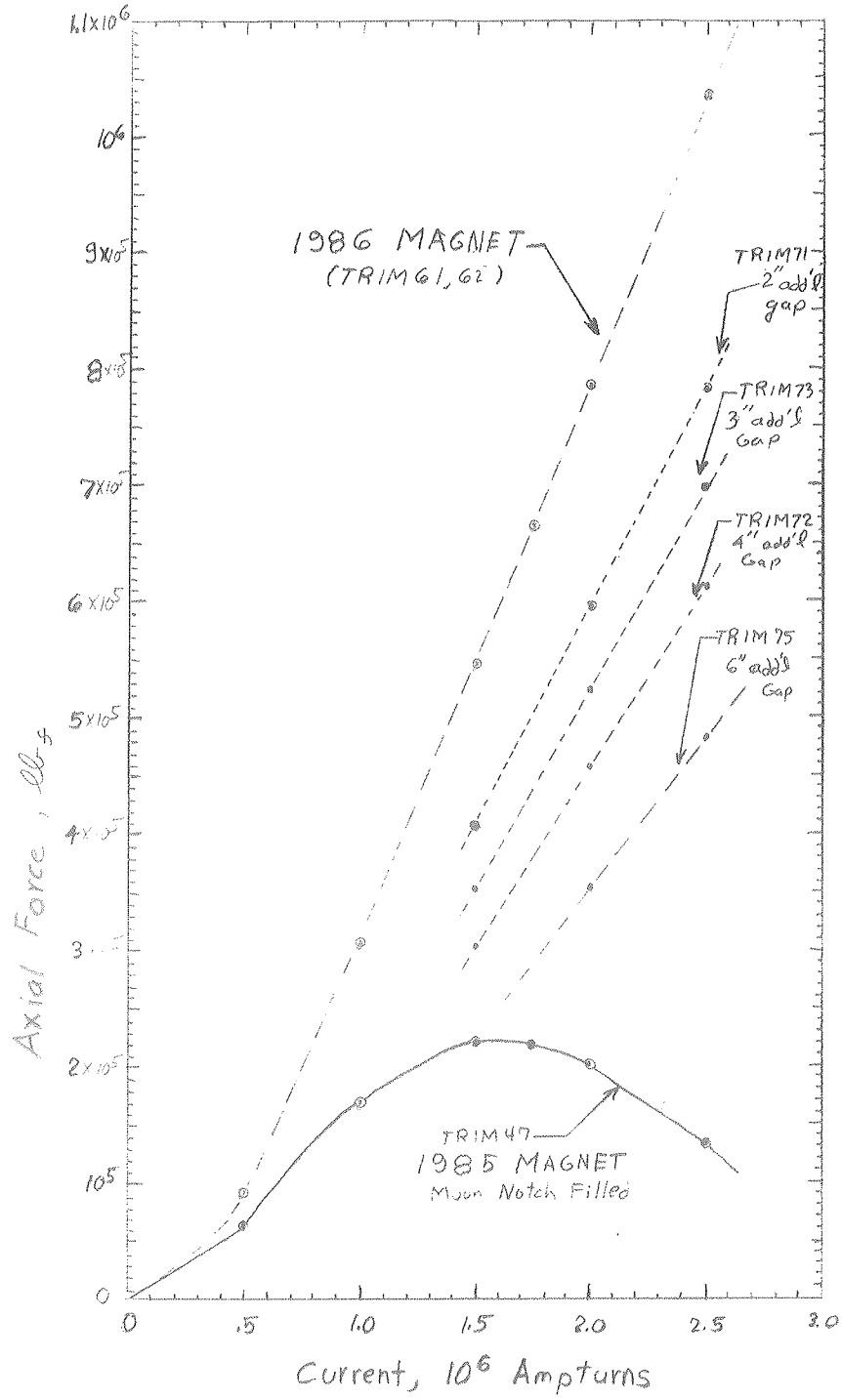

Figure 11: Axial force on coil versus current for the different magnets.

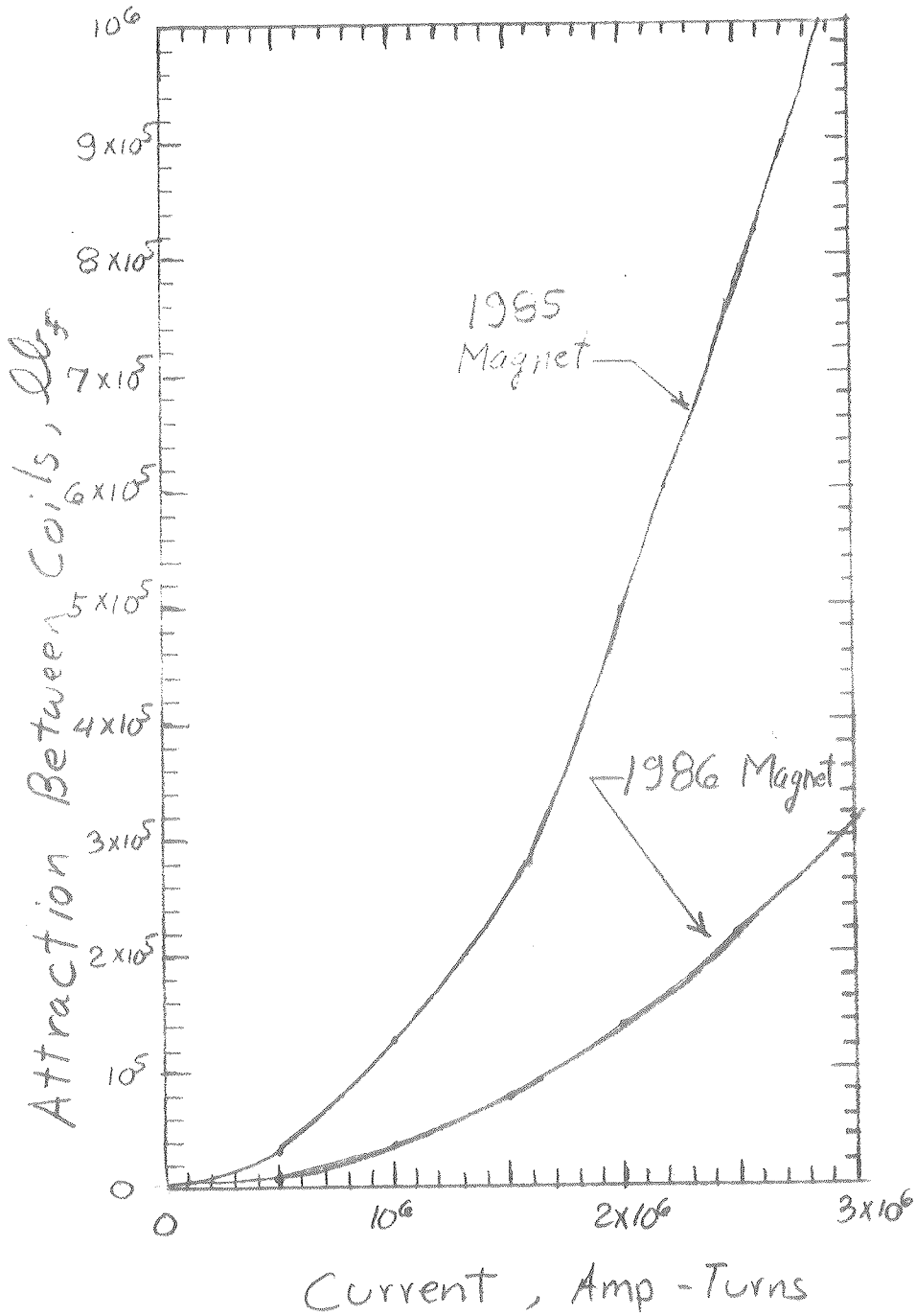

Figure 12: Attraction between coils as a function of current.

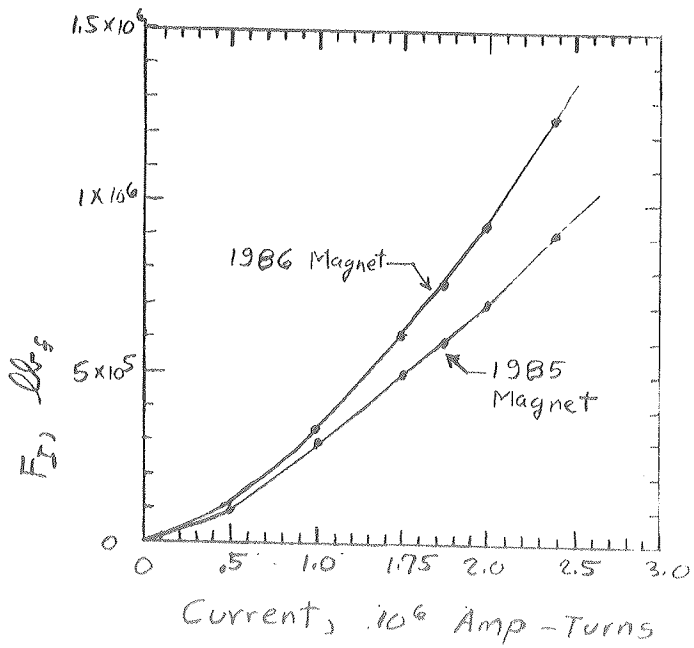

Figure 13: The attraction between a coil and the iron F_I, versus current. The inter coil attraction is not included in this example.

nearby iron having the cross section given in Fig. 5. Since this iron has cylindrical symmetry near the coils, it follows that the computer calculations for the axial force should be fairly accurate and were not greatly affected by the assumptions of cylindrical symmetry.

The axial force on the coil is not uniformly distributed over the coil and its supports. For the 1986 magnet with 6″ additional gap, Fig. 15 has, as a function of radius, the expected pressure distribution of the axial load over the outer surface of the coil. The pressures are much lower on the inside radius, because the hollow bore of the iron yoke exerts no attraction on the coil. For the same magnet, Fig. 16 is a plot of the electromagnetic axial force per turn as a function of Z for the inner, middle and outer radii of the coil. This force is approximately linearly distributed in the Z direction. It is negative at larger values of Z and positive at the smaller ones.

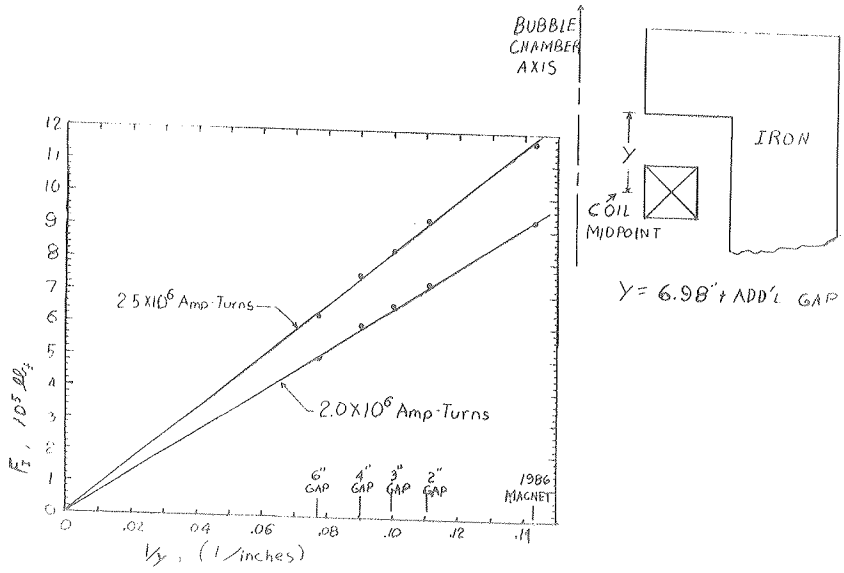

Figure 14: F_I versus $1/y$ for variations of 1986 Magnet.

Each coil is being compressed with a net force in the Z direction. The distribution of axial force per turn for the 1985 magnet is similar to Fig. 16, but the forces on individual turns are 10-20% lower, although the net axial force is about one-half. So, for the newer magnet, the the internal compressive axial forces inside the coil are a little worse.

The maximum internal compressive force between two turns can be estimated. The conductor was wound in layers, and each turn of a layer has the same radius. Consider Fig. 17, which shows one such layer. The rectangle a-b-c-d of this figure contains all of and only the turns of the layer with electromagnetic forces acting on them in the Z direction. Make an axial force balance on rectangle a-b-c-d. If friction between layers is ignored, the axial forces on surfaces a-b and c-d are 0. Also the axial force on surface d-a is 0, because the net axial force on the coil is away from this surface. The axial force F_3 on surface b-c is then equal to the sum of the axial

electromagnetic forces on all turns inside a-b-c-d. Since the electromagnetic forces per turn are almost linearly distributed

$$F_3 = (F_1/2) \times N \ ,$$

where N is the number of turns inside a-b-c-d, and F_1 is the electromagnetic force on the turn shown in Fig. 17. If M is the number of turns in a layer, then because of the linearity:

$$N = \left(\frac{F_1}{F_1 + F_2}\right) M \ ,$$

or

$$F_3 = \frac{F_1^2 M}{2(F_1 + F_2)} \ ,$$

where F_2 is the electromagnetic force on the turn shown in Fig. 17. For the 1986 magnet with an additional 6″ gap at the middle radius of 29.2″ (which is practically the worse case)

$$\begin{aligned} F_1 &= 2250 lb_f/turn \\ F_2 &= 2000 lb_f/turn \\ M &= 45^1 turns \end{aligned}$$

and

$$F_3 = 26,800 lb_f \ .$$

With the conductor thickness of .231 cm, the maximum axial compressive pressure is 1600 psi between turns. This is the maximum value, because if rectangle a-b-

[1] This was derived from the information in *Test Results and Design Details of the Tohoku Bubble Chamber Magnet*, W. Craddock, *et al.*, Vol. 31, Advances in Cryogenic Engineering, R.W. Fast, Editor, Plenum Press. The magnet was said to have 63 layers per coil, and to have operated at 1.99×10^6 Amp-turns per coil with 700 Amps. This implies that there are 2843 turns, and an average of 45 turns per layer.

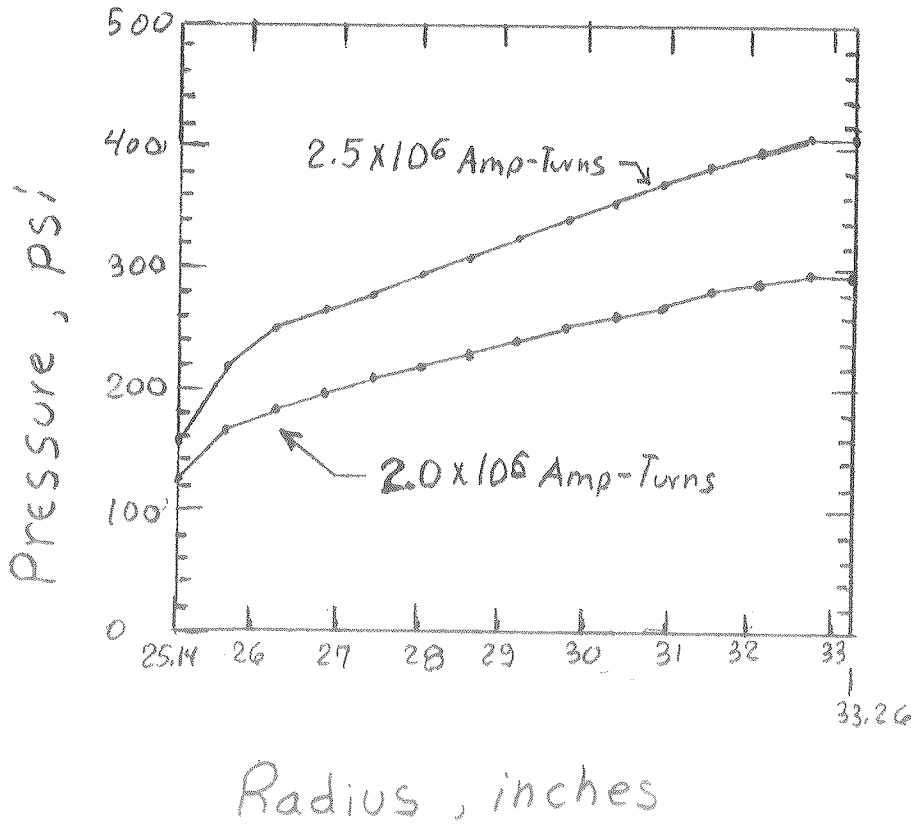

Figure 15: Pressure distribution of the 1986 magnet with 6″ additional gap over the coil supports.

c-d contained fewer turns with axial electromagnetic forces in the Z direction, F_3 would be less. Likewise, if rectangle a-b-c-d contained one or more turns with axial electromagnetic forces in the negative Z direction, then F_3 would be less.

It is of interest to know the axial magnetic spring constant, which is the change in axial force on the coil per unit axial motion of the coil. This was estimated by looking at the two components of the axial force. For the attraction between the coils in Appendix A, the force for a 1/4″ increase in the distance between the coils

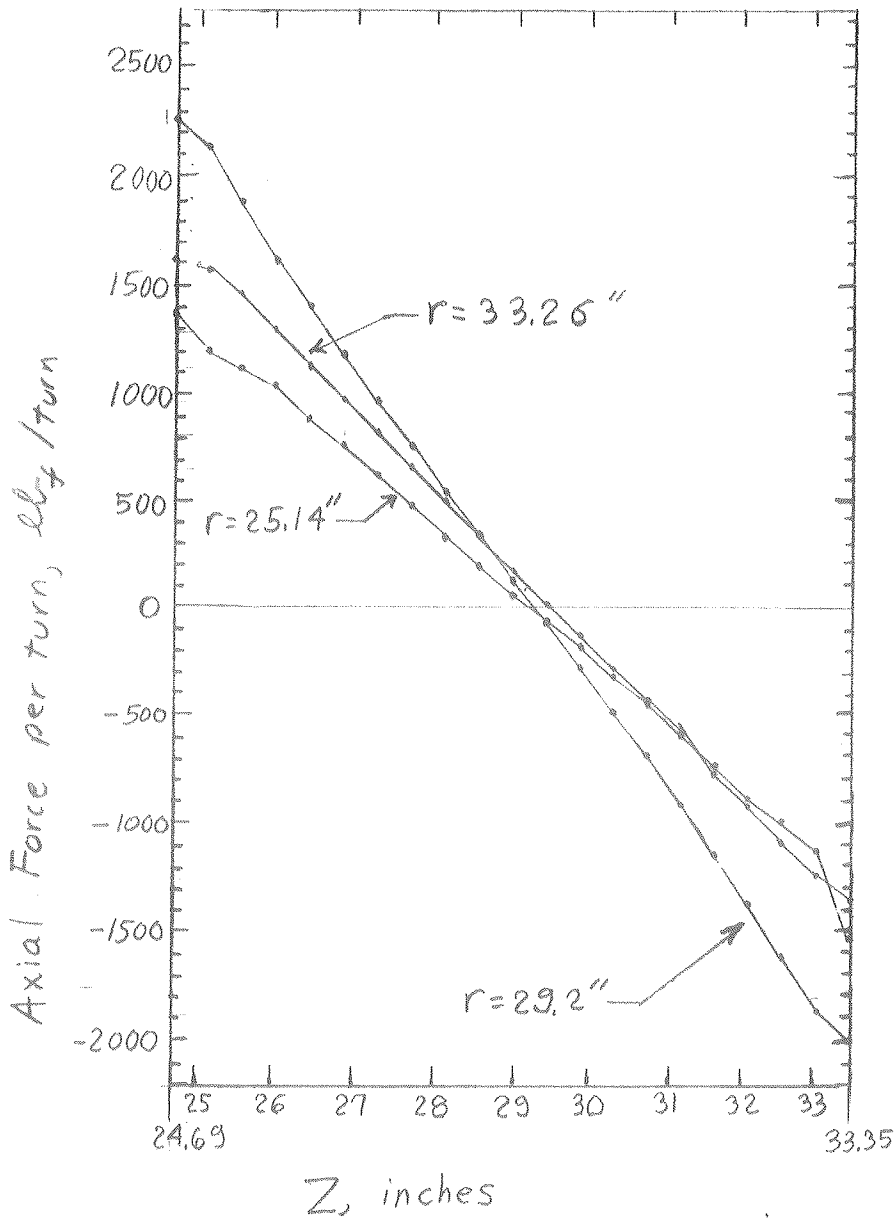

Figure 16: Axial force distribution versus Z for the 1986 magnet with a 6″ additional gap at different radii.

was computed for the different currents, and the rate of change estimated. This was doubled since, if one coil moves by a small amount, the other coil could have the same motion in the opposite direction. The rate of change in the attractive force between the coil and the iron was determined by approximating an analytical relationship from Fig. 14 ($F_I \propto 1/y$) and differentiating it. For the 1986 magnet with a 6″ additional gap, the magnetic spring constant is 50,800 lb_f/in for 2×10^6 Amp-turns and 68,400 lb_f/in for 2.5×10^6. A sample calculation is done in Appendix B. For the 1985 magnet, the axial magnetic spring constant was estimated to be $2 \times 10^5 lb_f/in$.[2]

[2]Tohoku Bubble Chamber Magnet Field Calculations, by Wes Craddock, January 21, 1985, p. 3.

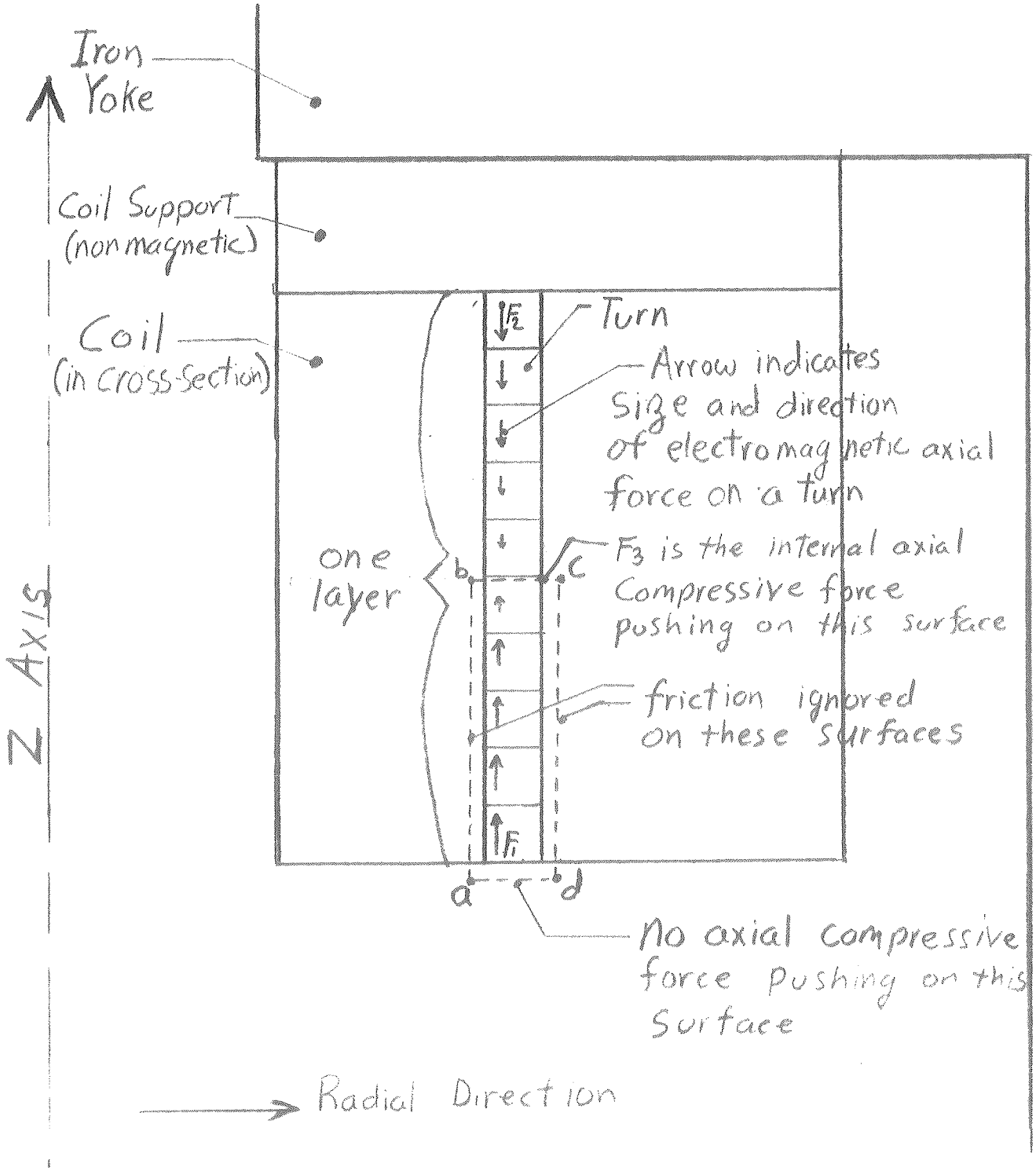

Figure 17: Sketch of a layer of conductor.

4 Radial Forces

The program FORGY gives the radial forces on the coil, in terms of circumferential hoop force the conductor would feel if it were completely rigid. The 1985 magnet had a calculated hoop force of 653,000 lb_f and the 1986 magnet, with a 6″ additional gap which will be the 1987 magnet, had a calculated 466,000 lb_f hoop force. The lower number for the newer magnet might be possibly caused by thinner return legs and the coils being farther apart. The greater axial separation from the iron might affect the hoop force as well. The exact magnitude of these calculated hoop forces should be viewed with some skepticism, because it is affected by the assumed cylindrical symmetry. However, the much smaller calculated value for the newer magnet implies that the radial decentering force and the radial magnetic spring constant will be, if anything, less than for the 1985 magnet.

Figure 18 has the axial distribution of hoop force per turn at the inner, middle, and outer radii of the 1987 magnet coil. The positive values of hoop force correspond to a positive radial force, pushing the conductor outwards while a negative hoop force is pushing it inwards. The coil is being compressed with a net radial force outwards. For the 1985 magnet, the calculated hoop force on individual turns was $\sim 20\%$ greater than for the new 1987 magnet.

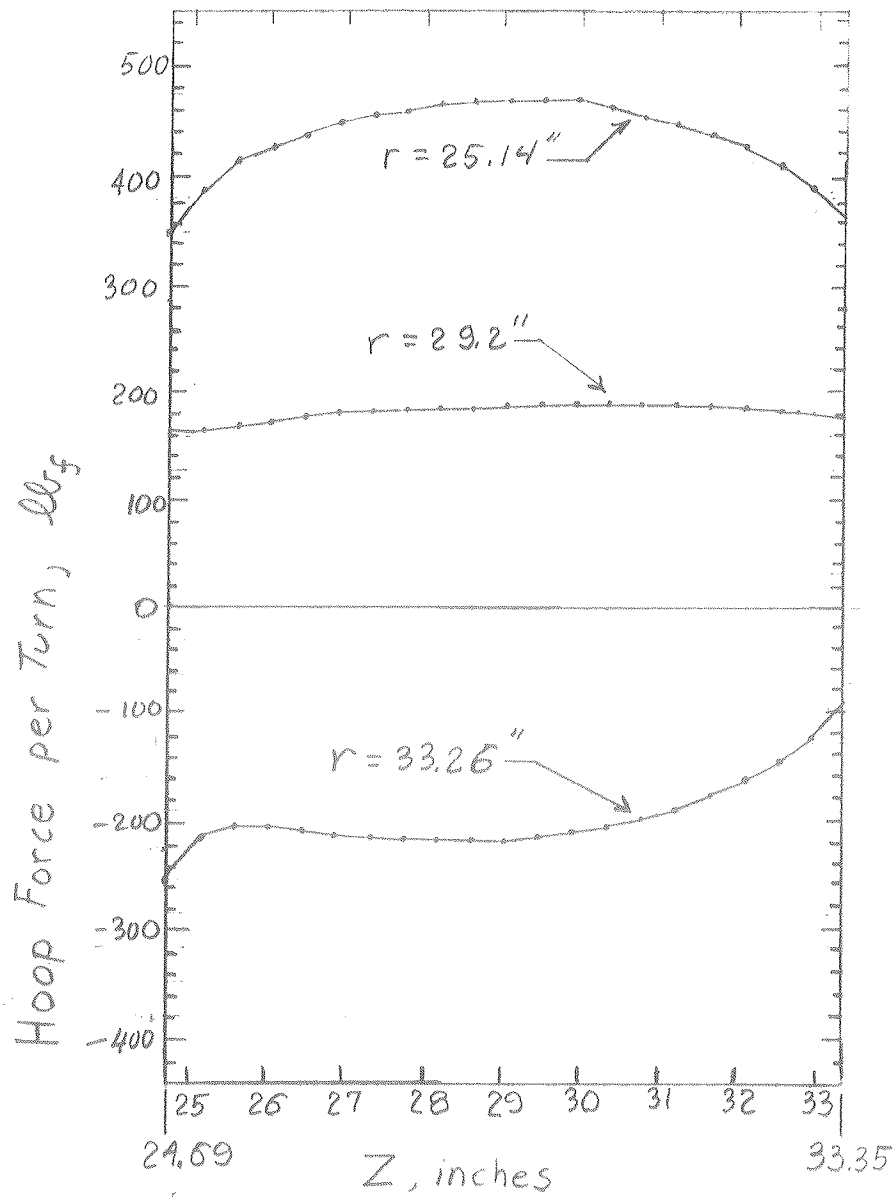

Figure 18: Hoop force per turn, as a function of Z at different radii for the 1986 magnet, with an additional 6″ gap. The current was 2×10^6 Amp turns.

5 Conclusions

The 1986 magnet was deemed unacceptable, because of the high 790,000lb_f axial force encountered at the 2×10^6 Amp-turn current required to achieve the desired central field of 15 KG. The modified 1986 magnet, with an additional 6″ gap, was selected to replace the 1986 magnet. This magnet, which will be used in 1987, gives the desired central field at a slightly higher 2.13×10^6 Amp-turn (750 Amp) current and a much smaller 390,000lb_f axial force than the 1986 magnet.

Since the 1986 magnet was never operated, it is better to compare the 1987 magnet to the 1985 magnet, which was successfully energized to 1.99×10^6 Amp-turns. In comparison, at its planned operating current of 750 Amps, the 1987 magnet will experience a higher (390,000lb_f versus 220,000lb_f) axial force, have the same stored energy (of about 10 MJ) and have a smaller axial magnetic spring constant (50,800lb_f/in versus 200,000lb_f/in). The axial compressive pressures inside the coil will be slightly higher ($\sim$ 20%) for the 1987 magnet, but will still be quite small with a maximum value of 1600 psi between two turns. In addition, the calculated hoop force on the coil is lower for the 1987 magnet (466,000lb_f) than the 1985 magnet (653,000lb_f), which indicates a smaller radial decentering force and radial magnetic spring constant. In general, except for the axial forces, the 1987 magnet will be operating at about the same conditions or better than the 1985 magnet.

APPENDIX A Analytical Calculation of Coil to Coil Magnetic Attraction

The radial component B_ρ of the magnetic field for an ideal circular current, produced by a wire loop, is given by the equation:[3]

$$B_\rho(Z,\rho) = \frac{\mu}{2\pi} I \frac{Z}{\rho} [(\rho + a)^2 + Z^2]^{-1/2} \left[-K(k) + \frac{a^2 + \rho^2 + Z^2}{(a-\rho)^2 + Z^2} E(k) \right] ,$$

where Z is the axial distance from the circular current loop, and ρ is the radial distance from the axis of the current loop, and the variable a is the radius of the current loop. The functions $K(k)$ and $E(k)$ are the complete elliptic integrals of the first and second kinds, respectively. The modulus k is defined by

$$k^2 = \frac{4\rho a}{(\rho + a)^2 + Z^2} .$$

The axial force F_c, imposed by one coil on the other, is given by

$$F_c = 2\pi a I B_\rho(Z, a) ,$$

which is the cross product between the B field and the current vector times the length of the circular loop. The variable Z is set equal to the distance between the centers of the coils and for all magnets $a = 29.2''$. The following table lists the formulae for the magnets.

Magnet	Coil Separation Z	Formula
1985	$33.66''$	$F_c = 1.23 \times 10^{-7} I^2$
1986	$58.04''$	$F_c = 3.4905 \times 10^{-8} I^2$
1986 $+1/4''$ deflection	$58.29''$	$F_c = 3.4506 \times 10^{-8} I^2$

[3] P141 of *Electromagnetic Fields*, Vol. I, by Ernst Weber, John Wiley & Sons, Inc., 1950.

The units of F_c are lb_f, and the units of I are amp-turns. This last entry in the table is for the 1986 magnet, with the coils displaced $1/4''$ farther apart. This is used in Appendix B.

APPENDIX B Sample Calculation of Axial Magnetic Spring Constant

Consider the 1986 magnet with a 6″ additional gap operating at a current of 2×10^6 amp-turns. From Fig. 14, the analytical approximation can be made:

$$F_I = (6.43 \times 10^6)/y \ ,$$

with F_I in lb_f and y in inches. Differentiating:

$$\frac{dF_I}{dy} = -(6.43 \times 10^6)/y^2 \ .$$

Evaluating this at $y = 12.98''$

$$\frac{dF_I}{dy} = -38000 lb_f/in \ ,$$

which is the rate that the attraction between the coil and the iron changes as the coil moves towards the middle of the magnet.

By using the formula derived in Appendix A, the change in the attractive force F_c between coils for a 1/4″ increase in the distance between them can be calculated as

$$\Delta F_c = [3.4506 \times 10^{-8} - 3.4905 \times 10^{-8}][2 \times 10^6]^2 = 1596 lb_f \ ,$$

so the derivative is

$$\frac{dF_c}{dZ} \approx -\frac{1596}{1/4} = -6400 lb_f/in \ .$$

The magnetic spring constant is then

$$\begin{aligned} \frac{dF_Z}{dZ} &= -\frac{dF_I}{dy} - 2\frac{dF_c}{dy} \\ \frac{dF_Z}{dZ} &= 38000 + 2(6400) = 50800 lb_f/in \ . \end{aligned}$$